Provided for non-commercial research and education use.
Not for reproduction, distribution or commercial use.

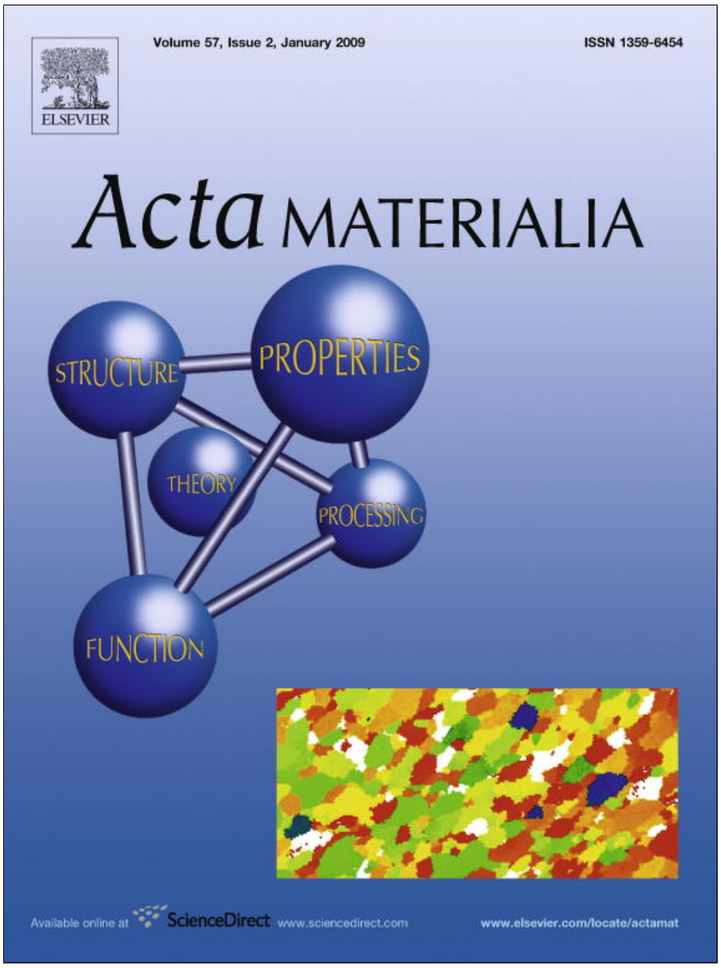

This article appeared in a journal published by Elsevier. The attached copy is furnished to the author for internal non-commercial research and education use, including for instruction at the authors institution and sharing with colleagues.

Other uses, including reproduction and distribution, or selling or licensing copies, or posting to personal, institutional or third party websites are prohibited.

In most cases authors are permitted to post their version of the article (e.g. in Word or Tex form) to their personal website or institutional repository. Authors requiring further information regarding Elsevier's archiving and manuscript policies are encouraged to visit:

http://www.elsevier.com/copyright

Author's personal copy

Available online at www.sciencedirect.com
ScienceDirect
Acta Materialia 57 (2009) 466–473
Acta MATERIALIA
www.elsevier.com/locate/actamat

Direct measurement of the variation in the energy of a dislocation locked in specific orientations

J. Douin *, P. Castany, F. Pettinari-Sturmel, A. Coujou

CEMES-CNRS, BP 94347, 28 rue Jeanne Marvig, 31055 Toulouse cedex 4, France

Received 7 May 2008; received in revised form 18 September 2008; accepted 20 September 2008
Available online 14 October 2008

Abstract

A general method is presented based on transmission electron microscopy observations of the segmented shape of dislocations under stress for measuring the decrease in dislocations' self-energy when they are locked in specific orientations. The general formulation is given for any direction of locking in any material, and the method is exemplified in the case of the hexagonal phases of an industrially important Ti-based alloy, where a significant in-core rearrangement reduces the energy of screw dislocations by ~16%.
© 2008 Acta Materialia Inc. Published by Elsevier Ltd. All rights reserved.

Keywords: Dislocations theory; Dislocations core structure; Energy calculations; Titanium alloys

1. Introduction

Obstacles to dislocation motion, which can be either intrinsic or extrinsic, dictate in many ways the mechanical behavior of material, as they control the dislocation mobility. Among numerous types of obstacles, the stabilization of dislocations along preferential directions plays a major role in plasticity: because they align along specific directions, dislocations have decreased mobility, thus providing a strong work-hardening mechanism. In particular, locking of dislocations along the screw orientation has been identified in numerous body-centered cubic (bcc) [1,2] or hexagonal close-packed (hcp) materials [3–5] as well as in ordered alloys [6,7] and diamond–cubic semiconductors [8,9] for example. This holds true for industrially important Ni-based alloys [10–12] or Ti alloys such as Ti–6Al–4V, which is the most commonly used Ti alloy in the aeronautic and aerospace industries [13–18].

The choice of the slip plane but also the stabilization of a dislocation along a given direction is often ascribed to the three-dimensional configuration of the dislocation core, and it is commonly admitted that atomic-scale computer modeling can provide much of the information required to study the core structure of dislocations. Indeed, modeling has revealed the variety of core states that can arise in different material, resulting in various slip plane choices. However, the reliability of atomic interactions may also be questionable in some areas. For example, rigorous density functional theory based calculations [19–21] are limited either to ideal structures or to the study of periodic arrays of very close-spaced defects. It has been shown that recently developed bond-order [22] and Finnis–Sinclair-type potentials [23,24] give qualitatively similar core structures for screw dislocations in basal or prism planes in pure titanium but predict opposite planes of spreading [25]. It is also worthwhile to point out that such modeling is generally made in stress-free conditions and/or at 0 K, and to emphasize that the simulation results highly depend on the initial assumptions and approximations. Thus, one of the most challenging aspects of material modeling is the choice of the description of atomic interactions that reflects the physical properties with sufficient accuracy. It is especially important in the case of locked dislocations as the intensity of the decrease in self-energy when the dislocations align along a specific direction is related to the

* Corresponding author. Tel.: +33 5 62 25 78 73; fax: +33 5 62 25 79 99.
E-mail address: joel.douin@cemes.fr (J. Douin).

1359-6454/$34.00 © 2008 Acta Materialia Inc. Published by Elsevier Ltd. All rights reserved.
doi:10.1016/j.actamat.2008.09.027

Author's personal copy

strength of the locking. For an applied stress smaller than the strength of the lock, the dislocations cannot overcome the obstacle and become locked in the stabilizing direction as soon as they attain the locking orientation: the segments in this direction lengthen, and the density of mobile segments decreases accordingly. The strength of the locking thus provides a stress limit to overcome for macroscopic deformation to be achieved.

Having a reliable experimental method for estimating the gain in energy when a dislocation locks for a given character would have two significant consequences: (i) it would allow the strength of locking of such an obstacle to be quantified for the dislocation motion and (ii) it would permit the calculated energy of a relaxed configuration to be related to the experimental energy, thus giving a constraint that simulations must fulfill in order to be representative of a defected crystal. Finally, it may also allow differentiation between different methods of numerical modeling or sets of data. It is the purpose of this paper to present a method based on transmission electron microscopy (TEM) observations allowing measurements of the relative variation in energy of a dislocation when it adopts a relaxed configuration in a specific direction. The general formulation will be given for any direction of stabilization and exemplified in the case of screw dislocations in the hexagonal phases of a Ti-based alloy.

2. Method of measurement of the relative variation in energy of a relaxed dislocation

Alignment of dislocations in specific orientations can be quite easily pointed out experimentally using TEM. In TEM observations, the locking of dislocations parallel to a direction results in a typical feature: long, straight segments of dislocations with a given character separated by curved segments (see, e.g., Fig. 1). Post mortem TEM observations provide a way to evidence such events by allowing large-scale observations of frozen dislocations. In situ TEM deformations give the additional possibility to observe dynamically the conditions of locking of moving dislocations in specific/preferential orientations and allows precise measurements of the physical parameters influencing the motion of dislocations: shape of moving segments, relative velocities or flight time of dislocations as a function of their character, for example [14,26,27].

The shape of a dislocation loop is given by the condition of minimum free energy E_t of the dislocation for a given stress. The parametric coordinates of a loop under a constant effective shear stress and for a friction stress independent of the dislocation character are given in Ref. [28]. Assuming isotropic linear elasticity, the shape of a dislocation loop is roughly an ellipsis (Fig. 2a and b), but it can deviate strongly from an ellipsis in the case of a strong crystalline anisotropy.

Anisotropic elasticity may indeed promote preferential orientations in cases, but the dislocations are then usually not strictly parallel to a specific direction [29] and deviate by as much as $\pm10°$ from the exact orientation. Then strict alignments of dislocations along a preferential direction cannot be usually ascribed to the influence of the anisotropy of the material. Rather, it attests to the stabilization of the dislocation resulting from an in-core relaxation, thus a decrease in self-energy, or equivalently a stronger friction stress, for this particular dislocation character. At the junction between locked straight segments and non-locked curved segments, the dislocation takes an angular shape. The angle φ at the cusp is characteristic of the strength of the stabilization in the locking direction, because the smaller the energy when stabilizing, the larger the φ. To relate the escape angle φ to the variation in energy implies

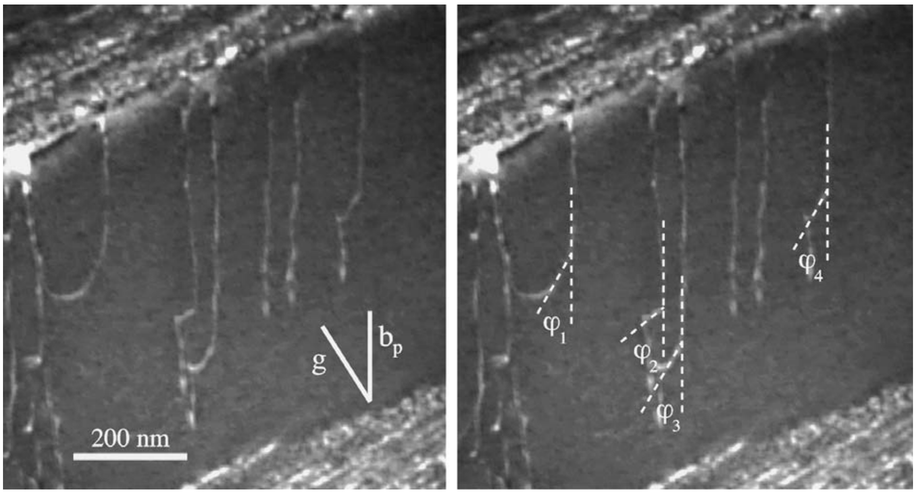

Fig. 1. In situ TEM weak-beam micrograph of $1/3\langle 11\bar{2}0\rangle$ dislocations extending in the (0001) basal plane of the α_s phase of a lamellar colony in the Ti–6Al–4V alloy. (a) The elongated part of the dislocations are aligned and locked along their screw orientation, attesting to an in-core relaxation of the dislocation line in this direction. b_p is the projection of the Burgers vector of the dislocations. (b) The same image as in (a), showing that, at the junction between screw and non-screw segments, the dislocation takes an angular shape with an angle φ_i at the cusp. Note that the angles φ_i are projected in the plane of the micrograph and must be corrected from this projection.

Author's personal copy

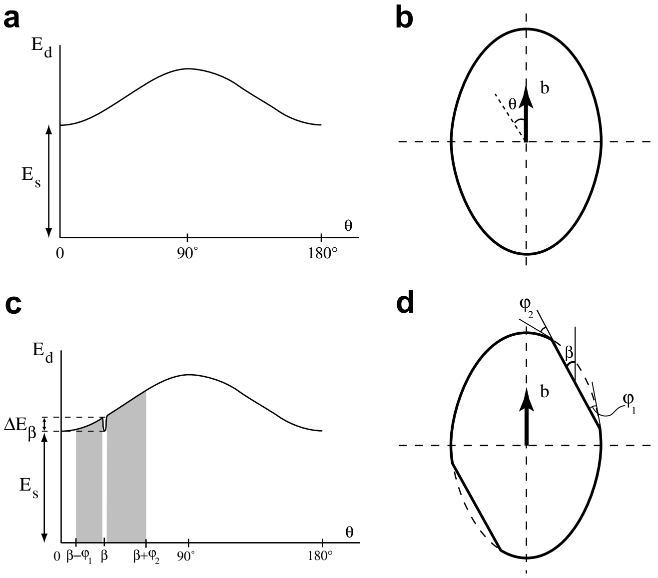

Fig. 2. Schematics of (a) the self-energy of a dislocation as a function of its character θ and (b) the corresponding shape of the dislocation loop under a constant shear stress. A special in-core rearrangement leading to a decrease ΔE_β in the self-energy of the dislocation for character β results in the formation of energetically unstable orientations (gray area in (c) limited by the angles $\beta - \varphi_1$ and $\beta + \varphi_2$), leading to a segmented shape for the dislocation loop (d).

computing the conditions of elastic stability of a dislocation loop and determining the changes induced by a decrease in the self-energy of the dislocation in a given direction.

Let ΔE_β be called the decrease in energy consecutive to an in-core rearrangement for a dislocation with character β (Fig. 2c). Such a decrease induces a modification of the shape of the dislocation at equilibrium, as it is energetically favorable for the dislocation to align along this orientation. Consequently, a characters domain exists of extent $\varphi_1 + \varphi_2$ for which dislocations become elastically unstable and which can be experimentally determined, as the angles φ_i can be measured by direct observations of cusped dislocations (Figs. 1 and 2d).

The determination of the general relation between angles φ_i and ΔE_β is reported in Appendix. In the case of anisotropic elasticity, the calculation cannot generally be done analytically but must be performed numerically. The simplest method for determining the escape angles is to calculate the conditions of stability of dislocation segments (through a Wulff plot; see Appendix), taking the decrease in energy in the stabilizing direction into account, then to measure the angles φ_i. This is exemplified in Fig. 3 in the case of a $[01\bar{1}]$ dislocation gliding in the (011) plane in NiAl. In this alloy, $\langle 110\rangle$ dislocations are locked in 35° directions [12]. The calculations were performed using the DISDI program [29,30], which is based on Stroh's formalism and uses a modified version of the Ancalc procedure [31]. Fig. 3 shows that the instability area extends from 14° to 67°, that is $\varphi_1 = 21°$ and $\varphi_2 = 32°$. It is important to notice that the calculated shape in Fig. 3b, assuming a relative decrease in energy of 10% in the 35° direction, is in very good accordance with TEM observations [12].

Assuming isotropic elasticity, an analytical relation exists between the relative variation in energy and the angles φ_i (see Appendix for the details of calculation):

$$\frac{\Delta E_\beta}{E_s} = 1 - \frac{(1-\nu)\cos\varphi - \nu(\cos^2(\beta\pm\varphi) + \cos(2\beta\pm\varphi))(1-\cos\varphi)}{1-\nu} \quad (1)$$

where $E_s = \mu b^2/(4\pi)\log(R/r_0)$ is the isotropic elastic energy of a screw dislocation with Burgers vector b, and μ, ν, R and r_0 are the usual elastic parameters [32]. φ_1 and φ_2 are solutions of Eq. (1) with sign $-$ and $+$, respectively.

An important and special case arises when stabilization occurs in the screw direction ($\beta = 0$) because, owing to symmetry, $\varphi_1 = \varphi_2 = \varphi$. The angle φ at the cusp is then the character of the curved segment tied to the elongated straight screw part of the dislocation. In this case, the relative variation in energy in the screw orientation $\Delta E_s/E_s$ is simply related to the escape angle φ by

$$\frac{\Delta E_S}{E_S} = 1 - \frac{(1-2\nu)\cos\varphi + \nu\cos^3\varphi}{1-\nu} \quad (2)$$

This relation allows the ratio $\Delta E_S/E_S$ to be estimated directly and accurately as a function of the measured angle φ.

Finally, it is worth pointing out that this method does not assume the origin of the stabilizing effect, which can arise from a Peierls effect, but also from a local but directionally constrained dissociation, as for example in the case of Lomer or Lomer–Cottrel configurations [33–35].

3. Locking in the screw orientation: the example of a Ti–6Al–4V alloy deformed in situ at room temperature

In many crystals with hcp structure and, in particular, in pure titanium and titanium alloys, deformation is performed by motion of **a**-type $1/3\langle 11\bar{2}0\rangle$ dislocations gliding in basal (0001) and/or prism $\{10\bar{1}0\}$ planes. The screw dislocations, lying parallel to the $\langle 11\bar{2}0\rangle$ direction, can spread into either of these planes or into both of them simultaneously. As it appears that it is energetically favorable for the dislocations to align strictly along their screw orientation, the screw dislocations have a particularly low mobility and control the activity of $1/3\langle 11\bar{2}0\rangle$ slip.

The Ti–6Al–4V under study has a duplex structure with primary hcp nodules (α_p) and lamellar colonies. The nodules and lamellar colonies have a similar size of ~10 μm in diameter. The lamellar colonies are constituted of layers of secondary hcp laths (α_s) separated by thin bcc β laths. As the β phase represents less than 3% in volume fraction, deformation occurs mainly in the hcp grains, even if the presence of this phase noticeably influences the mechanical properties of the alloy. The two hcp phases α_p and α_s have slightly different compositions, owing to an element partitioning effect during processing: the α_p phase has a higher concentration of α-stabilizer elements as aluminum or

Author's personal copy

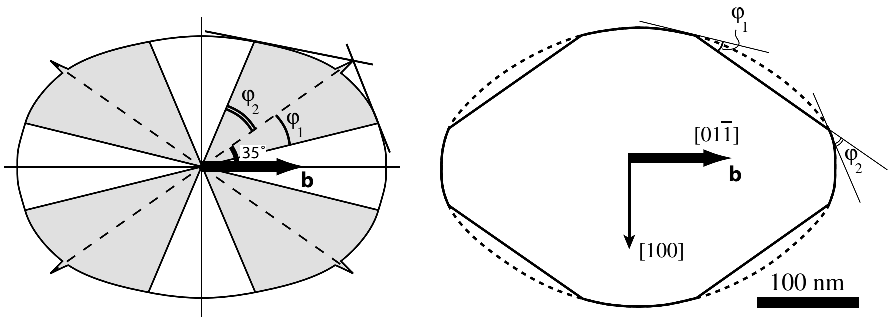

Fig. 3. (a) Wulff plot (arbitrary unit) showing the areas of elastically unstable orientations (in gray, limited by angles $\beta - \varphi_1$ and $\beta + \varphi_2$, with $\varphi_1 = 21°$ and $\varphi_2 = 32°$) for a [0 1 1] dislocation gliding in the (0 1 1) plane in NiAl and stabilizing at $\beta = 35°$ from the screw orientation ($\Delta E/E = 10\%$). (b) Corresponding shape (see Ref. [12] for comparison) The dashed line corresponds to the shape predicted by anisotropic elasticity (applied stress is 30 MPa).

oxygen than the α_s phase has [36]. Interestingly, in this alloy all gliding dislocations have the same **a**-type of Burgers vector, and prism and basal planes are the main slip planes observed in both α_p and α_s [14,15]. As in numerous hexagonal alloys, dislocations in the two α phases of Ti–6Al–4V adopt a clear preferential orientation along the exact screw orientation.

Figs. 1, 4 and 5 present examples of dislocations moving in the basal plane of α_s laths and basal and $(10\bar{1}0)$ prism planes of α_p nodules, respectively, during in situ experiments. Notice that no observation for prism glide in α_s laths is reported owing to the lack of observation of this glide system during the experiments, because it is slightly unfavored compared with the basal slip system in lamellar colonies [14,37]. The direct observations show that the dislocations keep the same shape during their motion and when they stop. The dislocations can be paired during their motion, owing to the presence of some short-range order (SRO) in the Ti–4Al–6V alloy [38], but this does not influence their shape.

Fig. 6 shows that, while favoring the screw character, elastic anisotropy is not responsible for such an alignment, thus the dislocations adopt a relaxed configuration in the screw orientation.

The escape angles were measured from in situ experiments for dislocations moving in either basal or prism planes. The angles were measured from the video-recorded images both by direct measurement and by fitting the shape of the dislocation with the computed one obtained from the DISDI program. Both methods gave the same results. As the glide plane of a moving dislocation is usually not the image plane where it is observed, the angle values have also been corrected to take their projection on the image plane into account, either by using a geometrical correction or by projecting the calculated shape from the glide plane to the image plane, again using the DISDI program. This was

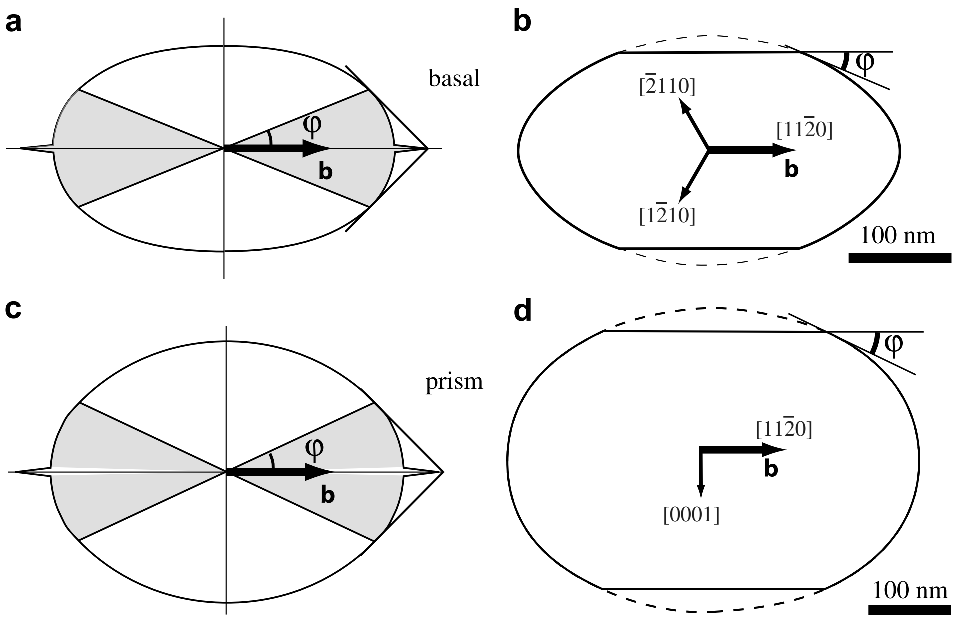

Fig. 4. (a) Wulff plot (arbitrary unit) showing the areas of elastically unstable orientations (in gray) for a **a**-type dislocation gliding in the basal plane of Ti–6Al–4V alloy and stabilizing in the screw orientation ($\delta E_s/E_s = 16\%$). (b) Corresponding shape of a dislocation loop (applied stress is 30 MPa). (c) and (d) Same for an **a**-type dislocation gliding in a prism plane. The dashed lines correspond to the shapes predicted by anisotropic elasticity.

Author's personal copy

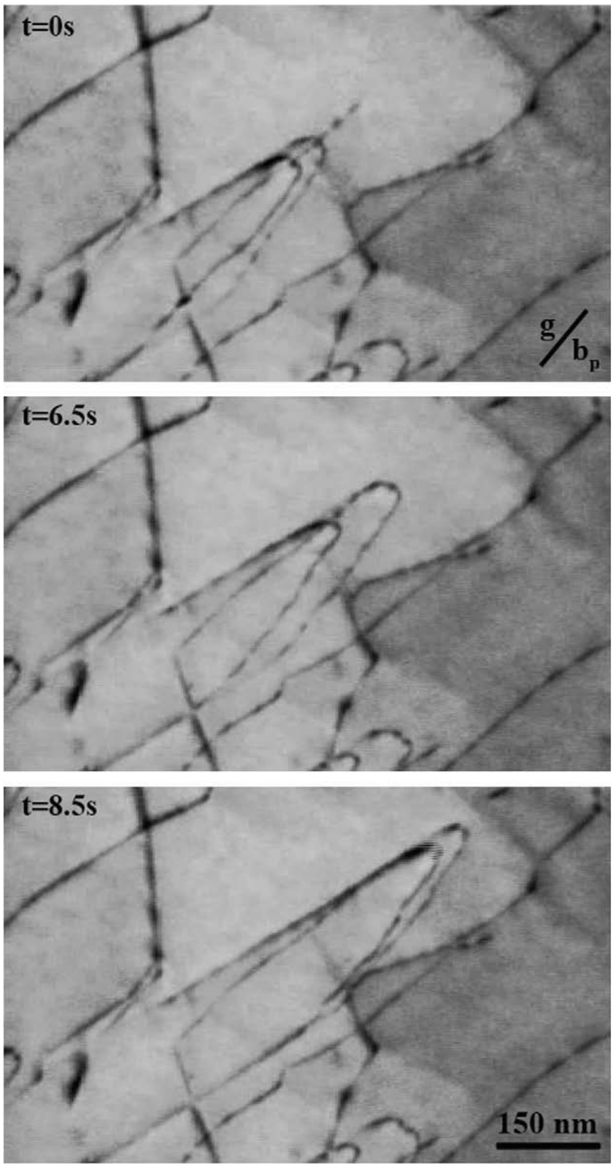

Fig. 5. In situ TEM sequence showing $1 = 3\ \langle 11\bar{2}0\rangle$ dislocations gliding in the basal plane of a ap grain of the Ti–6Al–4V alloy. The elapsed time for each observation is indicated. Dislocations are moving in pairs owing to the presence of SRO and keep a constant shape during their motion. b_p indicates the projection of their Burgers vector.

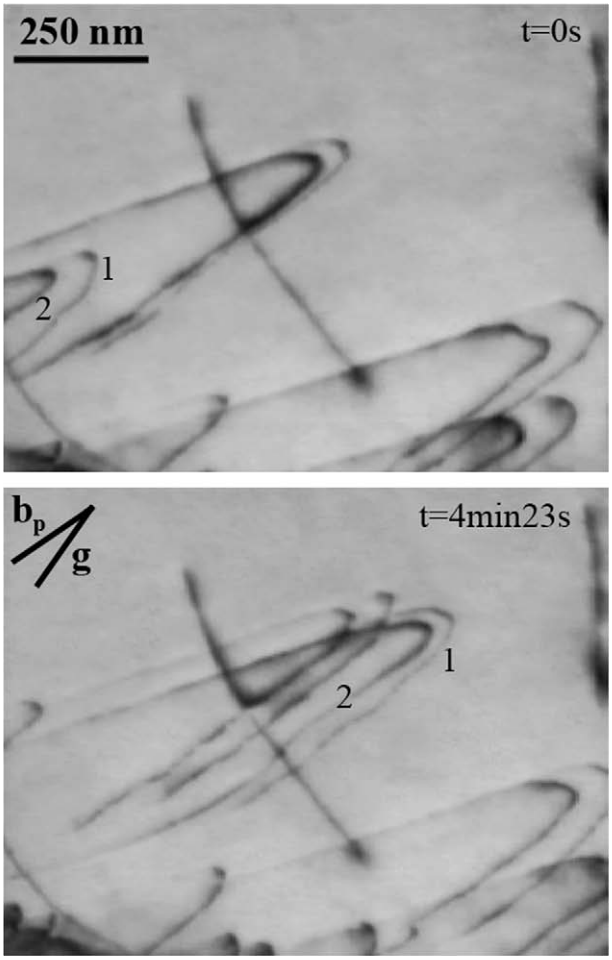

Fig. 6. In situ TEM observations showing $1 = 3\ \langle 11\bar{2}0\rangle$ dislocations gliding in the prismatic plane of a ap grain of the Ti–6Al–4V alloy at two different times. Dislocations noted 1 and 2 are moving in pairs owing to the presence of SRO and keep a constant shape during their motion. b_p indicates the projection of their Burgers vector.

made possible by experimentally determining both the glide plane of the dislocations and the observation plane, which is normal to the electrons beam. Care was also taken in choosing dislocation loops far from other dislocations as well as other sources of stress that would have locally modified the shape of the dislocations. However, this last point does not appear to be instrumental, as the shape of the dislocations does not change significantly during their motion if they are not crossing another dislocation.

The results of the escape angles measurements are reported in Fig. 7. It corresponds to ~50 different measurements of the escape angle during TEM in situ deformation experiments. From these measurements, the escape angles for the three observed glide configurations and the corresponding relative variation in energy in the screw orientation for the two phases were determined (Table 1). The calculations were made assuming isotropic and anisotropic elasticity, the latter using the elastic constants of Ti [39].

The low dispersion of the φ values attests to the good reproducibility of the measurements. As shown in Fig. 8, Eq. (2) assuming elastic isotropic catches fairly well the relative variation in energy if φ is <30°, which is almost always the case here. However, the escape angle is different for dislocations gliding in basal or prism planes in α_p nodules. This is simply due to different anisotropic behavior of the crystal in these two planes. As exemplified in Fig. 6, the elastic properties of a hexagonal crystal are different in the basal plane and in the prism planes, leading to a detectable difference for the escape angle, depending on the dislocation glide plane: for a relative variation in energy of 16%, there is a difference of ~3° for the escape angle, depending on the glide plane. In addition, the variation in energy is only dependent on the direction of the locking, not the glide plane, and accordingly the value of $\Delta E_s/E_s$ is found

Author's personal copy

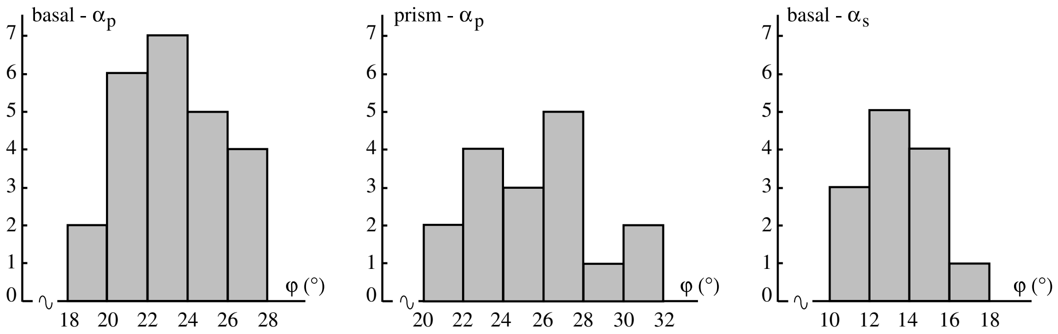

Fig. 7. Statistic of measurements of the escape angle φ from in situ experiments in the hcp phases of the Ti–6Al–4V alloy: (a) for basal glide in α_p nodule; (b) for prism glide in α_p nodule; (c) for basal glide in α_s lamella.

Table 1
Mean values of the escape angle φ determined using direct measurements in the hcp phases of the Ti–6Al–4V alloy and the corresponding decreases in energy (calculated assuming anisotropic elasticity)

α_p nodule	Basal glide	$\varphi = 23 \pm 5°$	$\Delta E_s/E_s = 0.165 \pm 0.07$
	Prism glide	$\varphi = 26 \pm 5°$	$\Delta E_s/E_s = 0.16 \pm 0.05$
α_s lath	Basal glide	$\varphi = 14 \pm 4°$	$\Delta E_s/E_s = 0.06 \pm 0.035$

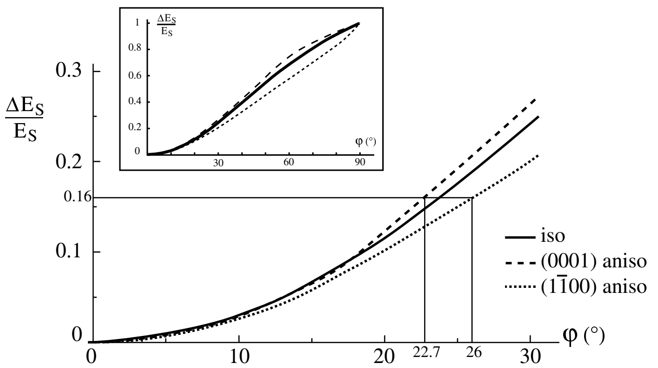

Fig. 8. Relative variation in the energy of a $1/3\langle 11\bar{2}0\rangle$ dislocation in Ti stabilized in the screw orientation as a function of the escape angle φ. The plain line was obtained using isotropic elasticity ($\nu = 0.248$), while dotted lines were calculated assuming anisotropic elasticity for dislocations moving in the (0001) basal plane and in the $(1\bar{1}00)$ prism planes (elastic constants of Ti: $C_{11} = 1.624$, $C_{12} = 0.92$, $C_{13} = 0.69$, $C_{33} = 1.87$ and $C_{44} = 0.467$ in 10^{11} Pa, from Ref. [39]). Notice that, for a given $\Delta E_s/E_s$, the escape angle φ is not the same for dislocations gliding in the basal plane and in a prism plane. Insert shows complete curve for φ ranging from 0° to 90°.

to be the same in α_p nodules, whether it is measured from dislocations gliding in basal planes or those gliding in prism planes (Fig. 8 and Table 1).

As no dissociation has been experimentally pointed out so far for screw dislocations in this alloy, such a high value of $\Delta E_s/E_s$ must be related to a significant but localized in-core rearrangement. Also, the relative reduction of energy $\Delta E_s/E_s$ is less pronounced in the α_s laths. This indicates that the stabilization in the screw orientation is softer in this phase and is in accordance with the fact that α_s has a lower concentration of alphagen elements and, in particular, interstitial elements such as oxygen, known to reduce the transition between sessile and glissile core structures [40].

Calculations show that the angles φ_i are only affected by the relative variation in energy when stabilizing, not by the effective stress acting on the dislocation, provided it can be locally considered as constant. In the particular case of the Ti–6Al–4V alloy, the existence of SRO has been pointed out in α_p nodules but not in the α_s laths [38]. SRO has a significant effect on the dislocation mobility by creating a strong friction stress. However, there is no experimental evidence in the alloy that the SRO friction stress differently affects segments of dislocations with different characters. Thus, the method of measurement remains valid here, and the fact that $\Delta E_s/E_s$ is smaller in the laths indicates that the locking in the screw orientation is really softer in this phase.

In the same vein, it is worth emphasizing that the method remains valid even for post mortem observations: in this case, the dislocation segments are frozen by equilibrating the back stress which tends to reduce the dislocation length, and the friction stress. Again, provided the friction stress acting on non-stabilized segments is independent of the character of the dislocation, the escape angles are representative of the variation in energy of the relaxed configuration.

4. Conclusions

It is possible to measure precisely the relative variation in energy of dislocations when they are locked in specific directions. The method is based on TEM observations of the shape of dislocations and can be applied for any stabilizing orientations and any materials, provided the effect on the dislocations is observable, that is the dislocations align spontaneously and significantly in specific directions. The method can be used to characterize the strength of a locking, thus give directions for alloy design, but also as a tool to help validate or calibrate atomistic simulations of dislocation cores.

In the Ti–6Al–4V alloy, the relative decrease in energy is close to 16% for screw dislocations gliding in basal or prism

Author's personal copy

planes in α_p nodules. Such a high value is related to a significant in-core relaxation of the screw dislocations. In the α_s laths, the relative reduction in energy $\Delta E_s/E_s$ is $\sim$6%, resulting from a softer but still noticeable stabilization in the screw orientation in this phase.

Appendix. Method of measurement of the relative variation in energy of a dislocation stabilized in a specific orientation

The shape of a dislocation loop is given by the condition of minimum free energy E_t for a given stress. Assuming linear elasticity, the stress is proportional to the deformation, which corresponds to a given area S of the loop. The shape of the loop will then be given by the condition that minimizes E_t assuming constant S. In what follows, the self-interaction between dislocation segments is neglected, as the influence of the self-interaction has been proved to be negligible provided the dimensions of the loop are not too small (see, e.g., Ref. [41]). If $E(\theta)$ is the self-energy by unit length of the segment of dislocation with character θ. The coordinates of the loop under a constant effective shear stress τ are given by [28]

$$x = \frac{1}{\tau b}\left(\cos(\theta)E(\theta) - \sin(\theta)\frac{\partial E(\theta)}{\partial \theta}\right)$$
$$y = \frac{1}{\tau b}\left(\sin(\theta)E(\theta) + \cos(\theta)\frac{\partial E(\theta)}{\partial \theta}\right)$$

where b is the modulus of the Burgers vector of the dislocation. It is worth pointing out that the shape of a dislocation is scaled when the local stress τ changes.

The conditions of stability regarding self-energy of a dislocation segment are determined using the inverse Wulff plot [42,43]. Take a dislocation segment, with length L, directed along the unitary vector $\vec{u}$. This segment will be considered unstable if it is energetically favorable to transform it into two connected segments with directions $\vec{u}_A$ and $\vec{u}_B$ and lengths L_A and L_B according to Fig. A1a.

The continuity of the dislocation implies

$$L \cdot \vec{u} = L_A \cdot \vec{u}_A + L_B \cdot \vec{u}_B$$

and the segment $\vec{u}$ will be energetically unfavorable if

$$LE > L_A E_A + L_B E_B$$

where E, E_A and E_B are the self-energies by unit length of the three segments. The limit of stability is given by the segment along $\vec{u}_P$, with length L_p and energy E_p, such that

$$L_p E_p = L_A E_A + L_B E_B$$

and

$$L_P \cdot \vec{u}_P = L_A \cdot \vec{u}_A + L_B \cdot \vec{u}_B$$

Let us find the location of the point P in the inverse plot of the self-energy of a dislocation segment as a function of its character, in polar coordinates (the so-called inverse Wulff plot). In this plot, the points A, B and P are given by

$$\vec{OA} = \frac{\vec{u}_A}{E_A}, \quad \vec{OB} = \frac{\vec{u}_B}{E_B} \text{ and } \quad \vec{OP} = \frac{\vec{u}_P}{E_P}$$

then

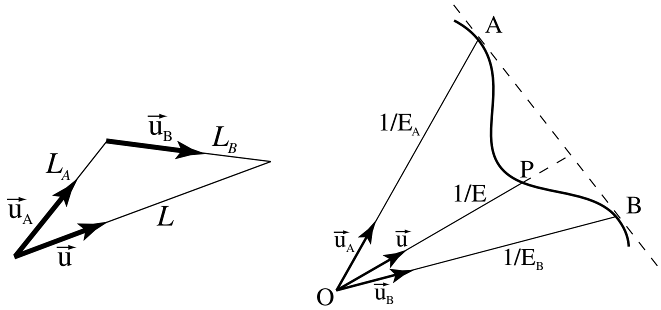

Fig. A1. (a) Schematic of the geometry of an angular configuration of dislocation. (b) Inverse Wulff plot revealing the orientation limits of dislocation stability.

$$\vec{OP} = \frac{L_P \cdot \vec{u}_P}{L_A \cdot E_A + L_B \cdot E_B}$$
$$(L_A \cdot E_A + L_B \cdot E_B)\vec{OP} = L_A \cdot E_A\vec{OA} + L_B \cdot E_B\vec{OB}$$
$$L_A \cdot E_A\vec{AP} = L_B \cdot E_B\vec{PB}$$

Notice that if $L_A \cdot E_A\vec{AP} = L_B \cdot E_B\vec{PB}$, the points A, B and P are aligned. Consequently, a direction $\vec{u}$ is stable if its corresponding point P is not located between segment AB and the origin of the curve. A direction $\vec{u}$ is unstable otherwise. The instability area for dislocation directions is then given by the contact points of the tangent of the inverse Wulff plot, $1/E$ in polar coordinates, which delimitates the concave area of the curve. Accordingly, the shape of the dislocation loop is modified, as there is a forbidden domain of orientations for the dislocation, and a cusp is created on the dislocation line, when the dislocation direction changes abruptly from $\vec{u}_A$ to $\vec{u}_B$.

In the case of a decrease in energy ΔE_β for the orientation β, resulting from an in-core relaxation or a special dissociation in this orientation, for example, a spike in the inverse Wulff plot ($E^{-1}(\theta)$ in polar coordinates) is created, which induces two instability areas corresponding to the concave parts of the plot (Fig. A2).

The slopes γ_1 and γ_2 at the limits of the instability areas are given by

$$\mathrm{tg}\,\gamma_\pm = \frac{\frac{\sin\beta}{E(\beta)-\Delta E_\beta} - \frac{\sin(\beta\pm\varphi)}{E(\beta\pm\varphi)}}{\frac{\cos\beta}{E(\beta)-\Delta E_\beta} - \frac{\cos(\beta\pm\varphi)}{E(\beta\pm\varphi)}}$$

where the sign $-$ or $+$ of γ corresponds to φ_1 and φ_2, respectively. The slopes γ are also given by

$$\mathrm{tg}\,\gamma_\pm = \frac{\mathrm{d}y}{\mathrm{d}x} = \frac{\partial\frac{\sin(\beta\pm\varphi)}{E(\beta\pm\varphi)}}{\partial\frac{\cos(\beta\pm\varphi)}{E(\beta\pm\varphi)}}$$
$$= -\frac{\cos(\beta\pm\varphi)E(\beta\pm\varphi) - \sin(\beta\pm\varphi)\frac{\partial E(\beta\pm\varphi)}{\partial(\beta\pm\varphi)}}{\sin(\beta\pm\varphi)E(\beta\pm\varphi) + \cos(\beta\pm\varphi)\frac{\partial E(\beta\pm\varphi)}{\partial(\beta\pm\varphi)}}$$

Equating the two expressions above leads to the value of ΔE_β, provided the expression of the self-energy $E(\theta)$ is known, either in isotropic or anisotropic elasticity. Then

Author's personal copy

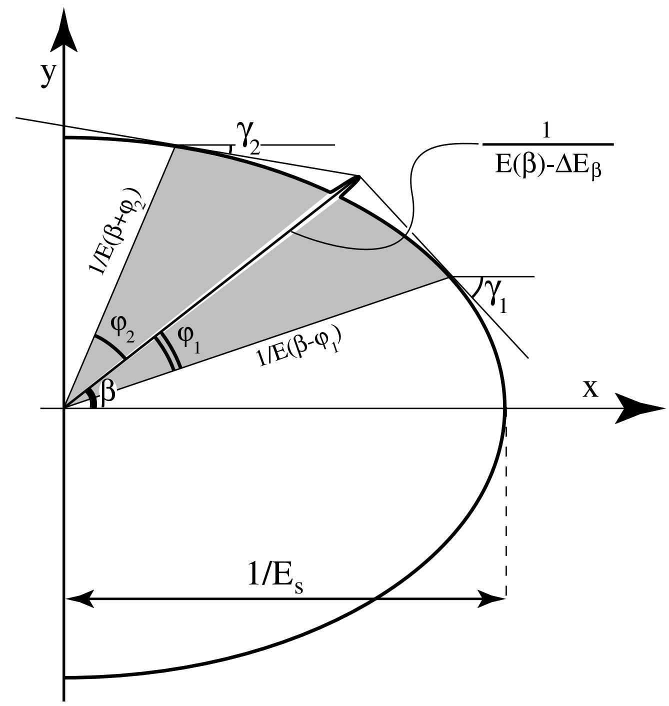

Fig. A2. Schematic inverse Wulff plot in the case of the stabilization of a dislocation in orientation β. The gray areas indicate the domains of dislocation lines instability resulting from the existence of a decrease in energy in orientation β.

the measurement of the angles φ would directly give the decrease in energy resulting in the stabilization of a dislocation in direction β. This calculation can be made for anisotropic elasticity but only numerically in most cases (see, e.g., Figs. 3 and 4).

Assuming isotropic elasticity, the self-energy by unit length of a segment of dislocation with character θ is given by Hirth and Lothe [32]

$$E(\theta) = \frac{\mu b^2}{4\pi}\left(\cos^2\theta + \frac{\sin^2\theta}{1-v}\right)\log\left(\frac{R}{r_c}\right)$$

where μ, v, R and r_c are the usual elastic parameters. If one calls E_s the energy of a screw dislocation, the relative variation in energy in the direction β is written

$$\frac{\Delta E_\beta}{E_s} = 1 - \frac{(1-v)\cos\varphi - v(\cos^2(\beta\pm\varphi)+\cos(2\beta\pm\varphi))(1-\cos\varphi)}{1-v}$$

In the special case of a stabilization of the dislocation in the screw orientation ($\beta = 0$), the symmetry implies $\varphi_1 = \varphi_2 = \varphi$, and the above expression reduces to

$$\frac{\Delta E_s}{E_s} = 1 - \frac{(1-2v)\cos\varphi + v\cos^3\varphi}{1-v}$$

The two instability domains are now symmetrical around the screw orientation, and the angle φ is the character of the non-screw segment of dislocation at the cusp.

References

[1] Hirsch P. Proceedings of the fifth international conference on crystallography. Cambridge: Cambridge University Press; 1960. p. 139.
[2] Christian J. Metal Trans A 1983;14:1237.
[3] Jonsson S, Beuers J. Mater Sci Eng 1987;91:111.
[4] Couret A, Caillard D. Philos Mag A 1989(59):783.
[5] Couret A, Caillard D, Pushl W, Schoeck G. Philos Mag A 1991;63:10450.
[6] Douin J, Veyssière P. Philos Mag A 1991;64:807.
[7] Veyssière P, Douin J. In: Intermetallic compounds: vol. 1. Principles. Chicester: John Wiley; 1994. p. 519.
[8] Wessel K, Alexander H. Philos Mag 1977;35:1523.
[9] Rabier J, Cordier P, Tondellier T, Demenet JL, Garem HJ. Phys Condens Mater 2000;12:10059.
[10] Veyssière P, Douin J, Beauchamp P. Philos Mag A 1985;51:469.
[11] Veyssière P, Saada G. In: Nabarro FRN, Duesbery MS, editors. Dislocations in solids, vol. 10. Amsterdam: North Holland; 1996p. 253.
[12] Yang N, Sun YQ. Acta Mater 2004;54:5615.
[13] Eylon D, Seagle SR. In: Gorgnin IV, Ushkov SS, editors. Titanium'99: science and technology, St. Petersburg, Russia; 2000. p. 37.
[14] Castany P, Pettinari-Sturmel F, Crestou J, Douin J, Coujou A. Acta Mater 2007;55:6284.
[15] Neeraj T, Hou DH, Daehn GS, Mills MJ. Acta Mater 2000;48:1225.
[16] Suri S, Viswanathan GB, Neeraj T, Hou DH, Mills MJ. Acta Mater 1999;47:1019.
[17] Welsch G, Bunk W. Metal Trans A 1982;13:889.
[18] Zaefferer S. Mater Sci Eng A 2003;344:20.
[19] Pettifor DG, Cottrell AH, editors. Electron theory in alloy design. London: The Institute of Materials; 1992.
[20] Finnis MW. Interatomic forces in condensed matter. Oxford: Oxford University Press; 2003.
[21] Finnis M. Prog Mater Sci 2004;49:1.
[22] Aoki M, Nguyen-Manh D, Pettifor DG, Vitek V. Prog Mater Sci 2007;52:154.
[23] Finnis MW, Sinclair JE. Philos Mag A 1984;50:45.
[24] Ackland GK, Tichy G, Vitek V, Finnis MW. Philos Mag A 1987;56:735.
[25] Girshick A, Pettifor DG, Vitek V. Philos Mag A 1998;77:999.
[26] Farenc S, Caillard D, Couret A. Acta Metall Mater 1993;41:2701.
[27] Benyoucef M, Clément N, Coujou A. Philos Mag A 1995;72:1043.
[28] Hazzledine PM, Karnthaler HP, Korner A. Phys Stat Sol (a) 1984;81:473.
[29] Douin J, Veyssière P, Beauchamp P. Philos Mag A 1986;54:375.
[30] The Disdi program is available for free at http://www.cemes.fr/Personnel/douin/Disdi-Page.html.
[31] Head AK, Humble P, Clareborough LM, Morton AJ, Forwood CT. Computed electron micrographs and defects identification. Amsterdam: North Holland; 1973.
[32] Hirth JP, Lothe J. Theory of dislocations. New York: Wiley; 1982.
[33] Lomer WM. Philos Mag 1951;42:1327.
[34] Cottrell AH. Philos Mag 1952;43:645.
[35] Bonneville J, Douin J. Philos Mag Lett 1990;62:247.
[36] Lütjering G. Mater Sci Eng A 1998;243:32.
[37] Ambard A, Guétaz L, Louchet F, Guichard D. Mater Sci Eng A 2001;404:319–21.
[38] Pettinari-Sturmel F, Castany P, Douin J, Coujou A., submitted for publication.
[39] Fisher ES, Renken CJ. Phys Rev 1964;135:A482.
[40] Naka S, Lasalmonie A, Costa P, Kubin LP. Philos Mag A 1988;57:717.
[41] Korner A, Karnthaller HP. Phys Stat Sol 1983;A75:525.
[42] Frank FC. Metal surfaces structures, energies and kinetics. Metals Park, OH: American Society of Metals; 1963.
[43] Head AK. Phys Stat Sol (a) 1967;19:85.